JBC Papers in Press. Published on May 12, 2017 as Manuscript M116.771493
The latest version is at http://www.jbc.org/cgi/doi/10.1074/jbc.M116.771493

The zinc finger E-box-binding homeobox 1 (*Zeb1*) promotes the conversion of mouse fibroblasts into functional neurons

Long Yan[1,#], Yue Li[3,#], Zixiao Shi[1, 2,#], Xiaoyin Lu[1, 2,#], Jiao Ma[1, 2], Baoyang Hu[1], Jianwei Jiao[1]*, Hongmei Wang[1]*

[1]*State Key Laboratory of Stem Cell and Reproductive Biology, Institute of Zoology, Chinese Academy of Sciences, Beijing 100101, China;* [2]*University of Chinese Academy of Sciences, Beijing 100049, China;* [3] *Center of Reproductive Medicine, Department of Obstetrics and Gynecology, Peking University Third Hospital, Beijing 100191, China**

Running title: *Zeb1* promotes transdifferentiation from MEFs to neurons

* **To whom correspondence should be addressed:**
Dr. Hongmei Wang, Institute of Zoology, Chinese Academy of Sciences, 1 Beichen West Road, Chaoyang District, Beijing 100101, P. R. China; E-mail: wanghm@ioz.ac.cn; Tel: 86-10-64807187; Fax: 86-10-64807189;
Dr. Jianwei Jiao, Institute of Zoology, Chinese Academy of Sciences, 1 Beichen West Road, Chaoyang District, Beijing 100101, P. R. China; E-mail: jwjiao@ioz.ac.cn; Tel: 86-10-64806335; Fax: 86-10-64806335

[#] contributed equally to this work

Key words: transdifferentiation, *Zeb1*, fibroblasts, neurons.

Downloaded from http://www.jbc.org/ by guest on July 16, 2017

Copyright 2017 by The American Society for Biochemistry and Molecular Biology, Inc.

Abstract

The zinc finger E-box binding transcription factor *Zeb1* plays a pivotal role in the epithelial-mesenchymal transition (EMT). Numerous studies have focused on the molecular mechanisms by which *Zeb1* contributes to this process. However, the functions of *Zeb1* beyond EMT remain largely elusive. Using a transdifferentiation system to convert mouse embryonic fibroblasts (MEFs) into functional neurons via the neuronal transcription factors Achaete-scute family bHLH transcription factor1 (*Ascl1)*, POU class 3 homeobox 2 (POU3F2/*Brn2*) and Neurogenin 2 (Neurog2, *Ngn2*) (ABN), we found that *Zeb1* was up-regulated during the early stages of transdifferentiation. Knocking down *Zeb1* dramatically attenuated the transdifferentiation efficiency, whereas *Zeb1* overexpression obviously increased the efficiency of transdifferentiation from MEFs to neurons. Interestingly, *Zeb1* improved the transdifferentiation efficiency induced by even a single transcription factor (e.g., *Asc1* or *Ngn2)*. *Zeb1* also rapidly promoted the maturation of induced neuron (iN) cells to functional neurons and improved the formation of neuronal patterns and electrophysiological characteristics. iN cells could form functional synapse in vivo after transplantation. Genome-wide RNA arrays showed that *Zeb1* overexpression up-regulated the expression of neuron-specific genes and down-regulated the expression of epithelial-specific genes during conversion. Taken together, our results reveal a new role for *Zeb1* in the transdifferentiation of MEFs into neurons.

Downloaded from http://www.jbc.org/ by guest on July 16, 2017

Introduction

The direct conversion of mouse embryonic fibroblasts (MEFs) into functional neurons (induced neurons, or iN cells) by Wernig and colleagues through the forced expression of the transcription factors Achaete-scute family bHLH transcription factor1 (*Ascl1*), POU class 3 homeobox 2 (POU3F2/*Brn2*) and myelin transcription factor 1 like (*Myt1l*) (ABM) was truly groundbreaking (1). These authors then systematized their research through a series of studies in which they directly converted human non-neural somatic cells (fetal and postnatal fibroblasts) and pluripotent stem cells into iN cells using the same three factors (2), induced human embryonic stem cells (ESCs) and induced pluripotent stem cells (iPSCs) into functional neurons by the forced expression of a single transcription factor (*Ngn2* or Neuronal differentiation 1 (*NeuroD1*)) (3), demonstrated the hierarchical mechanism of the three transcription factors and highlighted *Ascl1* as the single most important driver of reprogramming versus *Brn2* and *Myt1l*, which primarily enhanced neuronal maturation (4,5). Furthermore, this group found that *Ascl1* alone was sufficient to generate iN cells from mouse and human fibroblasts and from ESCs (6). A set of elegant studies from other laboratories also demonstrated that various combinations of transcription factors converted human fibroblasts into iNs (hiNs) or even specific neuronal subtypes, such as dopamine (hiDAs) and motor neurons (hiMNs) (2,7-10). Together with customized transcription factors, microRNAs, small molecules or even gene editing can be used to transdifferentiate MEFs into neurons (11-17). However, these studies largely utilized integrating delivery systems, such as retroviral or lentiviral vectors, which carried a high risk of introducing insertion mutations and activating tumor-related genes (18). Thus, we developed a non-integrating adenoviral delivery system and succeeded in converting fibroblasts into neurons by expressing a cocktail of transcription factors (*Ascl1*, *Brn2* and *Ngn2*-ABN) (18,19). This non-integrating system reduces the risk of insertion mutations and tumors, thereby providing new strategies for cell therapy for degenerative diseases and holding great promise for regenerative medicine. However, the efficiency of this approach is low, suggesting that additional transcription factors are needed to increase the conversion efficiency.

The ZEB (zinc finger E-box binding homeobox) family of transcription factors consists of two members, *Zeb1* (zinc finger E-box-binding homeobox 1) and *Zeb2* (also called Smad interacting protein 1, SIP1), both of which played pivotal roles in vertebrate embryonic development (20). As a well-known activator of the epithelial-mesenchymal transition (EMT), *Zeb1* has been extensively studied as a transcriptional repressor that negatively regulated the expression of the polarity marker E-cadherin (14,21-23). Extensive studies have also shown that *Zeb1* was also involved in cancer progression, facilitating tumor invasion and metastasis by driving the EMT (23-28). Furthermore, *Zeb1* has been implicated in the development of placental blood vessels, the palate, teeth and adipose tissue, and the DNA damage response (29-33). Homozygous *Zeb1* knockout (KO) mice have a cleft lip and palate, as well as aberrant proliferation and differentiation in chondroid tissues, and died within 24 h after birth (31). Interestingly, despite being a non-neuronal transcription factor, *Zeb1* played important roles in the nervous system during ontogenesis. For example, *Zeb1* was up-regulated in developing neurons in various parts of the central nervous system and is critical for the maintenance of spinal cord neural stem cells (34,35). Therefore, determining whether *Zeb1* functions during the conversion of fibroblasts into functional neurons is of great interest.

In this study, we used a non-integrating adenoviral delivery system expressing a combination of transcription factors (ABN) (18,19) to establish a transdifferentiation system for converting MEFs into functional neurons. Knocking down *Zeb1* in this system significantly decreased the transdifferentiation efficiency from fibroblasts to neurons, whereas *Zeb1* overexpression obviously increased the conversion efficiency, improved neuronal pattern formation, and enhanced the physiological functions of the iN cells. Furthermore, *Zeb1* overexpression increased the efficiency of transdifferentiation even in combination with individual A/N. Genome-wide RNA array analyses showed that *Zeb1* overexpression up-regulated the transcript levels of neuron-specific genes. Our findings provided the first evidence of a role for *Zeb1* in the production of iN cells via transdifferentiation.

Downloaded from http://www.jbc.org/ by guest on July 16, 2017

Results

Zeb1 was strongly up-regulated at early stages of ABN-mediated transdifferentiation-To examine the expression of *Zeb1* during the early stages of transdifferentiation from MEFs to functional neurons, primary MEFs were isolated from E13.5 mouse embryos, taking great care to exclude pre-existing neurons, astrocytes and neural progenitors (Fig S1A). We ectopically overexpressed the target genes using the commercial pAd-DEST adenoviral vector, whose backbone contains enhanced green fluorescent protein (eGFP) to facilitate the calculation of virus titers and the tracing of iN cells during transdifferentiation(18) (Fig 1A). MEFs were infected with ABN once daily for 2 consecutive days in transdifferentiation medium and then cultured in neuronal medium to promote neuronal survival and maturation until further analysis (Fig 1B). During culture in neuronal medium, MEFs were gradually induced into bipolar neuron-like cells, some of which even expressed the neuronal marker β-III-tubulin (*Tuj1*) 7 days post-infection (Fig 1C). iN cells became gradually mature as the culture period progressed (Fig 1C). Real-time PCR and Western blotting also showed that *Tuj1* levels were up-regulated over time, indicating the successful establishment of the transdifferentiation system (Fig 1D and Fig S1B). In conjunction with TUJ1 expression, ZEB1 protein levels increased during transdifferentiation. Both ZEB1 and TUJ1 reached their highest expression levels on day 4, and then their expression declined (Fig 1D). Consistent with the Western blot results, *Zeb1* mRNA was strongly up-regulated at the beginning of transdifferentiation, peaking on day 1 (Fig 1E).

Knocking down Zeb1 significantly decreased the transdifferentiation efficiency of MEFs into neurons by ABN-To test the functional role of *Zeb1* during transdifferentiation, we knocked down *Zeb1* in ABN-infected MEFs on day 2 post-infection using lentiviruses carrying either *Zeb1* shRNA or control shRNA (Fig 2A). The number of iN cells was counted based on immunofluorescence analysis of TUJ1 expression 7 days post-infection, while the conversion efficiency was calculated by dividing the number of iN cells (TUJ1 positive) by the number of total cells in each field (Fig 2C). The control groups (ABN alone or ABN plus control shRNA) showed almost equal numbers of TUJ1-positive cells (Fig 2 B and C). However, the number of TUJ1-positive cells was dramatically reduced in the *Zeb1* shRNA-infected group (Fig 2 B and C; $P < 0.01$).

Zeb1 promoted ABN-*mediated transdifferentiation from MEFs into neurons*-Encouraged by the above *Zeb1* knockdown results, we investigated the effect of *Zeb1* overexpression on transdifferentiation efficiency. We introduced the *Zeb1* adenovirus or the control adenovirus into MEFs infected with ABN. Seven days later, more TUJ1-positive cells were observed in the *Zeb1*-overexpressing MEFs, as demonstrated by immunostaining (Fig 3A). Statistical analyses showed that *Zeb1* overexpression promoted the conversion of MEFs into neurons by more than 3-fold compared with the control group (Fig 3B, $P < 0.01$). With the introduction of *Zeb1*, the ABN-treated MEFs started to exhibit neuronal morphology 3 days post-*Zeb1* infection, as determined by eGFP expression, whereas neuronal morphology was not observed in the control cells until 5 days after *Zeb1* infection (data not shown).

iN cells infected with ABN + *Zeb1* matured with prolonged cultivation (Fig S2A), and we observed some multipolar neurons in both the ABN and ABN + *Zeb1* groups after 3 weeks, with comparably more complex structures (Fig S2B).

Zeb1 promoted the generation of mature iN cells-Although the iN cells generated by ABN and *Zeb1* were TUJ1 positive and showed a neuronal morphology, it was necessary to evaluate the maturity of the iN cells. Immunostaining showed that the iN cells expressed mature neuronal markers 14 days post-infection, including the pan-neuronal markers microtubule-associated protein 2a (*Map2a*, 76.27% of the total iN cells; Fig 4A), neuronal nuclear protein (*NeuN*, 55.02% of the total iN cells; Fig 4B), and *Synapsin* (75.04% of the total iN cells; Fig 4C); the inhibitory neuron marker glutamate decarboxylase 1 (*GAD67*, 34.3% of the total iN cells; Fig 4D); the dopaminergic neuron marker tyrosine hydroxylase (*TH*, 20.25% of the total iN cells; Fig 4E); and the excitatory neuron marker vesicular glutamate transporter 1 (*vGLUT1*, 17.05% of the total iN cells; Fig 4F). We also tested the expression of these neuronal markers at other time points. On day 7 post-infection, only *Map2a*, *Synapsin* and *NeuN* were detected (Fig S3), but on day 21 post-infection, iN cells expressed all these neuronal markers we dected, with more complex structures (Fig S4). Next, we investigated whether

Downloaded from http://www.jbc.org/ by guest on July 16, 2017

Zeb1 could facilitate the maturation of iN cells at the physiological level. To examine the electrophysiological properties of the iN cells, such as the ability to fire action potentials (APs) and the induction of a membrane current, we performed whole-cell patch-clamp recording of iN cells with a complex neuronal morphology (eGFP-positive) on day 21 after adenovirus infection. Primary neurons were used as a positive control. Although depolarizing voltage steps in voltage-clamp mode elicited fast inward sodium currents in both the ABN- (Fig 5A) and ABN + *Zeb1* (Fig 5B)-induced iN cells, the latter appeared to exhibit better sodium and potassium currents that were more similar to those of primary neurons (Fig 5C). By contrast, we observed almost no consecutive APs in the ABN-infected iN cells 21 days post-infection (Fig 5A). Following *Zeb1* overexpression, however, the iN cells were able to fire multiple APs, similar to the primary neurons (Fig5 B and C). These results illustrated that *Zeb1* promoted maturation of iN cells and functional membrane properties.

Zeb1 facilitated the generation of iN cells induced by a single transcription factor-Previously, we found that the individual transcription factors *Ascl1*, *Brn2* or *Ngn2* were also able to mediate the reprogramming and conversion of MEFs into TUJ1-positive iN cells, although the process was slow and inefficient (data not shown). We therefore examined whether *Zeb1* in combination with A, B or N alone could improve the transdifferentiation efficiency. To address this question, we introduced *Zeb1* into A-, B- or N-infected MEFs. Although the transdifferentiation efficiency was 4.64%, 0.15% and 0.79% for A, B and N alone, respectively, *Zeb1* overexpression increased the efficiencies to 9.34% (Fig 6A, $P < 0.01$), 0.38% (Fig 6B) and 1.53% (Fig 6C, $P < 0.01$) in the A-, B- and N-treated groups, respectively. We also observed bipolar or multipolar iN cells after 3 weeks of cultivation in these groups (Fig S5). Interestingly, even *Zeb1* alone was able to convert MEFs into TUJ1-positive iN cells with more complex bipolar structures with the culture progressed (Fig S6).

iN cells formed functional synapse in vivo after transplantation-For accurate functional analysis of induced neurons, we transplanted ABN + *Zeb1*-induced iN cells (3 days post-infection) to the hippocampal area of 4-week-old C57BL/6 mice (Fig 7A). The mice which received grafts unilaterally were euthanized 3 weeks after transplantation, and the brain sections were collected for analysis. eGFP showed 2%-3% iN cells survived in the brain, after staining the brain sections with SYNAPSIN, we found some grafted iN cells labelled with GFP appeared extensive presynaptic innervation with other neurons (Fig 7B), suggesting the transplanted iN cells converted into neurons *in vivo*. Furthermore, we found the iN cells expressed other neuronal markers, such as *NeuN*, *GAD67* and *vGLUT1* (Fig 7C-7E), indicating the maturation of iN cells *in vivo*.

Zeb1 promoted primary neuron-like gene expression profiles in iN cells-To elucidate the molecular mechanism by which *Zeb1* promoted the transdifferentiation of MEFs into neurons following ABN induction, we examined genome-wide transcriptional changes in iN cells from days 1 to 7 post-infection using a genome-wide RNA array analysis. In this process, the genome expression patterns of both the ABN (Fig S7A) and ABN + *Zeb1* (Fig 8A) groups became increasingly similar to the primary neurons. However, in the ABN groups, the 5-day and 7-day profiles were more similar to the 3-day profile than to that of the primary neurons, whereas the 5-day and 7-day samples in the ABN + *Zeb1* groups tended to more closely mirror the primary neurons (Fig 8A and Fig S7A). During the conversion from MEFs to neurons, neuron-related genes such as *SYT1*, *PALM*, *Myt1l*, *NCAM*, *SYN2* and *SYN3* were significantly up-regulated (Fig 8B), whereas MEF-related genes such as *Snail1*, *FSP*1, *CD84*, *CD300*C, *COL1A1* and *GREM2* were markedly down-regulated (Fig 8B).

To explore the similarities in the genome-wide expression patterns of iN cells and primary neurons, we subjected all 14 samples (1-7 day ABN and 1-7 day ABN + *Zeb1*) to principle component analysis (PCA). The gene expression patterns of the iN cells showed progressively increasing differences from MEFs and a stepwise increase in similarity to the primary neurons over time. The 7-day ABN + *Zeb1* sample was closest to the positive control and showed a higher degree of similarity to the primary neurons than to the ABN sample (Fig S7B). Bioinformatic analysis identified 6,569 differentially expressed genes (DEGs, fold-change > 2, $P < 0.05$) in the ABN group and 6,600 DEGs in the ABN + *Zeb1* group compared with the control. Additionally, most DEGs (4,057 DEGs) from the 2 groups overlapped (Fig 8C). We then compared the

Downloaded from http://www.jbc.org/ by guest on July 16, 2017

2 DEG groups (7-day ABN and 7-day ABN + *Zeb1*). The up-regulated and down-regulated genes in 7-day ABN + *Zeb1* were subjected to Gene Ontology (GO) function enrichment analysis. Intriguingly, most up-regulated genes were enriched for GO terms associated with neuronal properties, such as signaling, neurological system process, and synapse or synaptic transmission, whereas most of the down-regulated genes were enriched in the GO terms related to MEF processes, including cellular process, regulation of biological process, cell periphery, and cell adhesion (Fig 8D).

To obtain a broad overview of the changes in transcript abundance over time, we performed Short Time-series Expression Miner (STEM) analysis. We found that a gene cluster continued growing over the 7-days cultivation (Fig S8 A and B). Then, we sent this cluster of 710 genes for GO analysis and found that these genes were mostly enriched for GO terms associated with neuronal processes, such as neuronal postsynaptic density, synaptic membrane, neuron-neuron synaptic transmission, and neuron cell body (Fig S8C).

Discussion

In this study, we used an adenovirus carrying *Zeb1* together with the defined non-integrating ABN transcription factors toconvert MEFs into neurons. *Zeb1* is not a traditional neuronal transcription factor. Here, we found for the first time that this non-neuronal transcription factor can promote the ABN-induced transdifferentiation of fibroblasts into neurons based on the following evidence. Firstly, knocking down *Zeb1* in the ABN inducing system significantly decreased the transdifferentiation efficiency. Conversely, the addition of *Zeb1* not only accelerated transdifferentiation but also improved the function of the induced neurons. Secondly, the ABN + *Zeb1*-induced neurons expressed specific neuronal markers, and they exhibited electrophysiological properties that were more similar to the primary neurons. More intriguingly, these iN cells further matured and formed functional synapses *in vivo* after being transplanted into hippocampal area of the mouse brain.

RNA array and bioinformatic analyses showed that the expression profiles of the ABN + *Zeb1* samples were more similar to primary neurons than the ABN groups and ABN + *Zeb1* could up-regulate neuron-related genes and down-regulate MEF-related genes to a greater degree than the ABN group. STEM analysis found that ABN + *Zeb1* up-regulated two more clusters of genes than ABN group, the function of these genes were “negative regulation of neuron apoptotic process” and “negative regulation of neuron death”, suggesting Zeb1 may improve the transdifferentiation by modulating apoptosis. *p53* was an important factor in programmed cell apoptosis, and it was recently reported that *p53* repressed *Zeb1* and *Zeb2* expression by up-regulating miRNAs, including miR-200 and miR-192 family members (37). Conversely, suppression of *p53* markedly increased the transdifferentiation efficiency of fibroblasts into induced dopaminergic neurons by *Ascl1*, *Nurr1*, *Lmx1a* and miR-124 (38). Thus, there may be a regulatory network between *Zeb1*, *p53* and neuron death regulating genes during transdifferentiation from MEFs into neurons, which requires further study.

Another interesting finding of this study is that *Zeb1* improved the transdifferentiation efficiency induced by single neuron transcription factors, *Ascl1* or *Ngn2*. *Ascl1* has been reported to be the driving force for iN cell reprogramming. MEFs transfected with *Ascl1* alone were fully reprogrammed to a neuronal lineage but were less mature at early time points and required further maturation by the introduction of two other transcription factors (*Brn2* and *Myt1l*) at later time points (4,6). Here, we found that *Zeb1* overexpression significantly improved *Ascl1*-mediated transdifferentiation. Other single transcription factors, such as *NeuroD1* or *Ngn2*, could facilitated differentiation from human/mouse ESCs or iPSCs into neurons, but can not mediate the transdifferentiation from fibroblasts to neurons (3,36). In our study, *Ngn2* alone was found to be able to promote transdifferentiation from fibroblasts to neurons, albeit with a relatively low efficiency, and that the addition of *Zeb1* greatly improved this efficiency. *Zeb1* could also promoted *Brn2*-activated transdifferentiation to some extent, although this effect was not statistically significant. This result was expected because *Brn2* is primarily required during later reprogramming stages to enhance neuronal maturation and is not deterministic for the neuronal lineage when expressed alone (6). Furthermore, we found even

Downloaded from http://www.jbc.org/ by guest on July 16, 2017

Zeb1 alone could initiate the transdifferentiation of MEFs into iN cells. It is a fascinating challenge to investigate the related mechanisms and elucidate whether *Zeb1* alone can transdifferentiate MEFs into mature and functional neurons.

In summary, our data revealed that *Zeb1* is a new and important transcription factor in transdifferentiation, it can promote the transdifferentiation from MEFs into iN cells more efficiently and functionally.

Experimental procedures

Animals-WT ICR mice, aged 6-8 weeks, 10 female (approximately 26 g) and 5 male (approximately 30 g), were purchased from Vital River Laboratory Animal Technology Corp (Beijing, China) and then raised in a sterile room. All experiments were performed under the guidance of the ethics committee of the Institute of Zoology, Chinese Academy of Sciences.

Isolation and culture of mouse embryonic fibroblasts (MEFs)-Primary MEFs were isolated from E13.5 ICR mouse embryos(1). First, the head, dorsal root ganglia, vertebral column, and visceral organs were removed; then, the remaining tissues were dissected into small pieces and treated with 0.25% trypsin (25200-056, Gibco) for 10 min. The dissociated cells were cultured in DMEM (11995-065, Gibco) supplemented with 10% fetal bovine serum (FBS) (Biochrom), 0.1 mM non-essential amino acids (NEAA) (11140-050, Gibco), and 2 mM Glutamax (35050-061, Gibco) in a 37°C and 5% CO_2 incubator. MEFs were used between passages 2 and 4.

Adenovirus production and infection-We used the Gateway Expression System (Invitrogen, Carlsbad, California, USA) to produce adenoviruses carrying the transcription factors *Ascl1*, *Brn2*, *Ngn2* or *Zeb1*, as described previously (18). The candidate genes were amplified from a mouse cDNA library and inserted into the pENTR 3C vector (Invitrogen, Carlsbad, California, USA). The resulting plasmids were generated by homologous L/R recombination. Viral constructs were transfected into 293A cells, and high-titer (10^8 IU/mL) viral particles were obtained by 2 rounds of amplification according to the manufacturer's instructions. The determination of the adenoviral titer was similar to that of the lentiviral titer except that the virus stock was diluted because the addition of a high concentration of adenovirus caused the majority of the 293T cells to die quickly. MEFs were infected twice with adenovirus for 8 h per day at a multiplicity of infection (MOI) of 10. Twenty-four hours later, half of the culture medium was changed to neural medium (Neural Basal/DMEM-F12 1:1, 1×B-27, 5 ng/ml BDNF). Afterwards, half of the medium was replaced every 2 days until the cells were ready for immunostaining and electrophysiological experiments.

Lentivirus production-Lentiviruses containing the different shRNAs were purchased from GenePharma, SuZhou. Control shRNA sequence: TTCTCCGAACGTGTCACGTTTC.
Zeb1 shRNA sequence:
GAAAGGCATTTAAACACAA;
GCAGTTACACCTTTGCATA;
GCCCACAGATACGACAGAA.

Immunofluorescence-iN cells were fixed with 4% PFA for 20 min at room temperature and then treated with 0.3% Triton X-100 for 10 min before being blocked with 5% BSA for 30 min. Primary antibodies were diluted in antibody dilution buffer (PBS with 1% BSA and 0.1% Triton X-100). The iN cells were incubated overnight with primary antibody at 4°C and treated with secondary antibody for 60 min at room temperature. The following primary antibodies were used: rabbit anti- TUJ1 (T3952, Sigma), mouse anti-MAP2a (MAB378, Millipore), mouse anti-NeuN (MAB377, Millipore), rabbit anti-TH (AB152, Millipore), rabbit anti-ZEB1 (ABN285, Millipore), mouse anti-GAD67 (MAB5406, Millipore), mouse anti-SYPSIN (106001, Synaptic Systems) and mouse anti-vGLUT1 (MAB5502, Millipore). The secondary antibodies were diluted 1:200 in ADS. The cells were washed with PBS and incubated with the appropriate highly cross-adsorbed Alexa Fluor 555 goat anti-rabbit IgG (A-21429, Life Technologies) and Alexa Fluor 647 goat anti-mouse IgG antibodies (A-21236, Life Technologies). Images were acquired on a Carl Zeiss LSM 780 confocal laser-scanning microscope with a 10× or 20× objective lens, and image analysis was conducted using the Zeiss LSM Image Browser software.

Transdifferentiation efficiency analysis-The conversion efficiency was quantified using the neuronal purity as the percentage of TUJ1 cells relative to the total final population. Briefly, eight to ten visual fields were randomly selected per well.

Downloaded from http://www.jbc.org/ by guest on July 16, 2017

The number of iN cells marked by TUJ1 staining and the number of total cells visualized by DAPI staining were counted. The efficiency was calculated by dividing the number of iN cells by the number of total cells in each field.

Quantitative PCR analysis-The transdifferentiated cells were harvested every 24 h. Total RNA was extracted using TRIzol (15596-018, Ambion) according to the manufacturer's instructions. Two micrograms of total RNA was reverse transcribed and then quantified using SYBR Green (RR820A, TaKaRa). β -actin was included as the reference. The sequences of the *Zeb1* primers were as follows:
Forward: 5'TGAGCACACAGGTAAGAGGCC3';
Reverse: 5'GGCTTTTCCCCAGAGTGCA3'.

Western blotting-Cells were lysed in RIPA buffer (50 mM Tris, pH 7.5, 150 mM NaCl, 0.1% SDS, 1% NP40, 2 mM EDTA and 0.5% sodium deoxycholate) supplemented with 1 mM phenylmethylsulfonyl fluoride and a protease inhibitor cocktail (Roche). Proteins were quantified using the BCA Protein Assay Kit (Pierce Biotechnology). Briefly, 20 μg of total protein extract was subjected to SDS-PAGE and transferred electrophoretically onto a pure nitrocellulose blotting membrane (Pall Corporation). After being blocked with 5% skim milk, the membrane was sequentially incubated with primary antibodies against ZEB1 (sc-25388, Santa Cruz), TUJ1 (T3952, Sigma) and β-actin (TA-09, ZSGB-Bio), followed by horseradish peroxidase-conjugated secondary antibodies. The signals were developed using the Gene Gnome Imaging System (Syngene Bio-imaging).

Electrophysiology-Electrophysiological experiments were performed on MEF-derived iN cells 7-12 days post-infection. Whole-cell patch-clamp recordings in either voltage- or current-clamp mode were conducted to measure voltage-activated sodium/potassium currents or action potentials and were recorded using an Axopatch 200B or MultiClamp 700A amplifier (Molecular Devices). The electric signals were filtered at 2-10 kHz, digitized at 20-100 kHz (Digidata 1322A; Molecular Devices) and analyzed using pClamp version 9.2 (Molecular Devices). The glass micropipette contained a solution consisting of 130 mM K^+-gluconate, 20 mM KCl, 10 mM HEPES, 0.2 mM EGTA, 4 mM Mg_2ATP, 0.3 mM Na_2GTP and 10 mM Na^{2+}-phosphocreatine (at pH 7.3, 310 mosmol), and the pipette ranged from 2.0 to 4.0 MΩ. The bath solution contained 124 mM NaCl, 3.3 mM KCl, 2.4 mM $MgSO_4$, 1.2 mM NaH_2PO_4, 26 mM $NaHCO_3$ and 10 mM glucose (at pH 7.4, 310 mosmol). The transmitter receptor blockers tetrodotoxin (100 nM), AP5 ((*2R*)-amino-5-phosphonovaleric acid, 50 μM) and CNQX (6-cyano-7-nitroquinoxaline-2, 3-dione, 10 μM) were used in the bath solution for the detection of action potentials and spontaneous excitatory postsynaptic currents.

Transplantation of iN cells in vivo-5×10^4 iN cells were transplanted into the hippocampal area of 4-week-old C57BL/6 mice. Three weeks after transplantation, the mice were perfused with 0.9% saline and followed by 4% paraformaldehyde (PFA). The brains were dissected out and fixed in 4% PFA overnight, followed by dehydration in 15% sucrose for 1 day at 4℃, then 30% sucrose for 1 day at 4℃. Consecutive coronal sections (30 μ m) were prepared using a Leica CM 1950 Sliding Microtome.

Gene expression microarray analysis-The mouse genome-wide gene expression analysis was performed using HOA Gene chips (Phalanx Biotech Group, Inc.). Total RNA was extracted from primary MEFs, from MEFs infected with adenoviruses carrying ABN or ABN + *Zeb1* at different days post-infection and from primary hippocampus neurons from a postnatal day 0 ICR mouse (a positive control). RNA was reversed transcribed using SuperScript II Reverse Transcriptase (18064-014, Invitrogen). For gene expression profiling analysis, the MouseWG-6 v2.0 Expression BeadChip Kit was used, which contains 26,423 mouse genome probes and 872 experimental control probes. The Rosetta Resolver System (Rosetta Biosoftware) was used to calculate the GeneChip Robust Multichip Average and to normalize the data sets for the single-channel experiment analyses. PCA was performed using SPSS V. 19. Hierarchical clustering analysis was applied using a Euclidean distance matrix and the complete-linkage clustering method. Linear models and empirical Bayes methods were used to choose DEGs that showed > 2-fold changes and an adjusted *P* value less than 0.05. Afterwards, DEGs with expression level changes > 2-fold were applied for GO analyses using DAVID Bioinformatics Resources.

Downloaded from http://www.jbc.org/ by guest on July 16, 2017

Statistical analysis-Statistical analysis was performed using Student's *t*-test with a paired, 2-tailed distribution. Values were considered statistically significant at $P < 0.05$ (*) and $P < 0.01$ (**). All data represent the mean ± S.D. or S.E., as detailed in the figure legends.

Acknowledgements: This work was supported by the "Strategic Priority Research Program" of the Chinese Academy of Sciences (XDA01020102). We are very grateful to the Beijing Compass Biotechnology Company for their excellent technical assistance with the microarray experiments.

Conflict of interest: The authors declare that they have no conflicts of interest with the contents of this article.

Author contributions: H.W. conceived the study, designed the experiments, and supervised the research. J.J. conceived the study and critically revised the manuscript. L.Y., Y.L., Z.S. and X.L. conducted the experiments and analyzed the data. L.Y. and Y.L. collected and analyzed the data, organized figures and drafted the manuscript. Z.S. and X.L. contributed to the adenoviral vector construction and the figure organization. J.M. contributed to the immunofluorescent experiments. B.H. conceived the study and commented on the manuscript. All authors contributed to the figure and manuscript preparation and approved the version that was submitted.

Downloaded from http://www.jbc.org/ by guest on July 16, 2017

References

1. Vierbuchen, T., Ostermeier, A., Pang, Z. P., Kokubu, Y., Südhof, T. C., and Wernig, M. (2010) Direct conversion of fibroblasts to functional neurons by defined factors. *Nature* **463**, 1035-1041
2. Pang, Z. P., Yang, N., Vierbuchen, T., Ostermeier, A., Fuentes, D. R., Yang, T. Q., Citri, A., Sebastiano, V., Marro, S., Sudhof, T. C., and Wernig, M. (2011) Induction of human neuronal cells by defined transcription factors. *Nature* **476**, 220-223
3. Zhang, Y., Pak, C., Han, Y., Ahlenius, H., Zhang, Z., Chanda, S., Marro, S., Patzke, C., Acuna, C., Covy, J., Xu, W., Yang, N., Danko, T., Chen, L., Wernig, M., and Sudhof, T. C. (2013) Rapid single-step induction of functional neurons from human pluripotent stem cells. *Neuron* **78**, 785-798
4. Wapinski, O. L., Vierbuchen, T., Qu, K., Lee, Q. Y., Chanda, S., Fuentes, D. R., Giresi, P. G., Ng, Y. H., Marro, S., Neff, N. F., Drechsel, D., Martynoga, B., Castro, D. S., Webb, A. E., Sudhof, T. C., Brunet, A., Guillemot, F., Chang, H. Y., and Wernig, M. (2013) Hierarchical mechanisms for direct reprogramming of fibroblasts to neurons. *Cell* **155**, 621-635
5. Ali, F. R., Cheng, K., Kirwan, P., Metcalfe, S., Livesey, F. J., Barker, R. A., and Philpott, A. (2014) The phosphorylation status of Ascl1 is a key determinant of neuronal differentiation and maturation in vivo and in vitro. *Development* **141**, 2216-2224
6. Chanda, S., Ang, C. E., Davila, J., Pak, C., Mall, M., Lee, Q. Y., Ahlenius, H., Jung, S. W., Sudhof, T. C., and Wernig, M. (2014) Generation of induced neuronal cells by the single reprogramming factor ASCL1. *Stem cell reports* **3**, 282-296
7. Pfisterer, U., Kirkeby, A., Torper, O., Wood, J., Nelander, J., Dufour, A., Bjorklund, A., Lindvall, O., Jakobsson, J., and Parmar, M. (2011) Direct conversion of human fibroblasts to dopaminergic neurons. *PNAS* **108**, 10343-10348
8. Caiazzo, M., Dell'Anno, M. T., Dvoretskova, E., Lazarevic, D., Taverna, S., Leo, D., Sotnikova, T. D., Menegon, A., Roncaglia, P., Colciago, G., Russo, G., Carninci, P., Pezzoli, G., Gainetdinov, R. R., Gustincich, S., Dityatev, A., and Broccoli, V. (2011) Direct generation of functional dopaminergic neurons from mouse and human fibroblasts. *Nature* **476**, 224-227
9. Ambasudhan, R., Talantova, M., Coleman, R., Yuan, X., Zhu, S., Lipton, S. A., and Ding, S. (2011) Direct reprogramming of adult human fibroblasts to functional neurons under defined conditions. *Cell stem cell* **9**, 113-118
10. Son, E. Y., Ichida, J. K., Wainger, B. J., Toma, J. S., Rafuse, V. F., Woolf, C. J., and Eggan, K. (2011) Conversion of mouse and human fibroblasts into functional spinal motor neurons. *Cell stem cell* **9**, 205-218
11. Ladewig, J., Mertens, J., Kesavan, J., Doerr, J., Poppe, D., Glaue, F., Herms, S., Wernet, P., Kögler, G., Müller, F.-J., Koch, P., and Brüstle, O. (2012) Small molecules enable highly efficient neuronal conversion of human fibroblasts. *Nature Methods* **9**, 575-578
12. Shenoy, A., and Blelloch, R. (2012) microRNA induced transdifferentiation. *F1000 Biology Reports* **4**
13. Chanda, S., Maro, S., Wernig, M., and Sudhof, T. C. (2013) NEURONS GENERATED BY DIRECT CONVERSION OF FIBROBLASTS REPRODUCE SYNAPTIC PHENOTYPE CAUSED BY AUTISM-ASSOCIATED NUuroligin-3 mutation. *PNAS* **110**, 16622-16627
14. Chang, Y. C., Tsai, C. H., Lai, Y. L., Yu, C. C., Chi, W. Y., Li, J. J., and Chang, W. W. (2014) Arecoline-induced myofibroblast transdifferentiation from human buccal mucosal fibroblasts is mediated by ZEB1. *Journal of cellular and molecular medicine* **18**, 698-708

Downloaded from http://www.jbc.org/ by guest on July 16, 2017

15. Hu, W., Qiu, B., Guan, W., Wang, Q., Wang, M., Li, W., Gao, L., Shen, L., Huang, Y., Xie, G., Zhao, H., Jin, Y., Tang, B., Yu, Y., Zhao, J., and Pei, G. (2015) Direct Conversion of Normal and Alzheimer's Disease Human Fibroblasts into Neuronal Cells by Small Molecules. *Cell stem cell* **17**, 204-212
16. Li, X., Zuo, X., Jing, J., Ma, Y., Wang, J., Liu, D., Zhu, J., Du, X., Xiong, L., Du, Y., Xu, J., Xiao, X., Wang, J., Chai, Z., Zhao, Y., and Deng, H. (2015) Small-Molecule-Driven Direct Reprogramming of Mouse Fibroblasts into Functional Neurons. *Cell stem cell* **17**, 195-203
17. Yoo, A. S., Sun, A. X., Li, L., Shcheglovitov, A., Portmann, T., Li, Y., Lee-Messer, C., Dolmetsch, R. E., Tsien, R. W., and Crabtree, G. R. (2011) MicroRNA-mediated conversion of human fibroblasts to neurons. *Nature* **476**, 228-231
18. Meng, F., Chen, S., Miao, Q., Zhou, K., Lao, Q., Zhang, X., Guo, W., and Jiao, J. (2012) Induction of fibroblasts to neurons through adenoviral gene delivery. *Cell research* **22**, 436-440
19. Shi, Z., Shen, T., Liu, Y., Huang, Y., and Jiao, J. (2014) Retinoic acid receptor gamma (Rarg) and nuclear receptor subfamily 5, group A, member 2 (Nr5a2) promote conversion of fibroblasts to functional neurons. *Journal of Biological Chemistry* **289**, 6415-6428
20. Gheldof, A., Hulpiau, P., van Roy, F., De Craene, B., and Berx, G. (2012) Evolutionary functional analysis and molecular regulation of the ZEB transcription factors. *Cellular and molecular life sciences : CMLS* **69**, 2527-2541
21. Liu, Y., El-Naggar, S., Darling, D. S., Higashi, Y., and Dean, D. C. (2008) Zeb1 links epithelial-mesenchymal transition and cellular senescence. *Development* **135**, 579-588
22. Fu, J., Lv, X., Lin, H., Wu, L., Wang, R., Zhou, Z., Zhang, B., Wang, Y. L., Tsang, B. K., Zhu, C., and Wang, H. (2010) Ubiquitin ligase cullin 7 induces epithelial-mesenchymal transition in human choriocarcinoma cells. *The Journal of biological chemistry* **285**, 10870-10879
23. Zhang, P., Sun, Y., and Ma, L. (2015) ZEB1: at the crossroads of epithelial-mesenchymal transition, metastasis and therapy resistance. *Cell cycle* **14**, 481-487
24. Arima, Y., Hayashi, H., Sasaki, M., Hosonaga, M., Goto, T. M., Chiyoda, T., Kuninaka, S., Shibata, T., Ohata, H., Nakagama, H., Taya, Y., and Saya, H. (2012) Induction of ZEB proteins by inactivation of RB protein is key determinant of mesenchymal phenotype of breast cancer. *The Journal of biological chemistry* **287**, 7896-7906
25. Berx, G., Raspe, E., Christofori, G., Thiery, J. P., and Sleeman, J. P. (2007) Pre-EMTing metastasis? Recapitulation of morphogenetic processes in cancer. *Clinical & experimental metastasis* **24**, 587-597
26. Yang, J., and Weinberg, R. A. (2008) Epithelial-mesenchymal transition: at the crossroads of development and tumor metastasis. *Developmental cell* **14**, 818-829
27. Ren, J., Chen, Y., Song, H., Chen, L., and Wang, R. (2013) Inhibition of ZEB1 reverses EMT and chemoresistance in docetaxel-resistant human lung adenocarcinoma cell line. *Journal of cellular biochemistry* **114**, 1395-1403
28. Sanchez-Tillo, E., Barrios, O., Siles, L., Cuatrecasas, M., Castells, A., and Postigo, A. (2011) β-catenin/TCF4 complex induces the epithelial-to-mesenchymal transition (EMT)-activator ZEB1 to regulate tumor invasiveness. *PNAS* **108**, 19204-19209
29. Pirinen, E., and Soini, Y. (2014) A survey of zeb1, twist and claudin 1 and 4 expression during placental development and disease. *APMIS : acta pathologica, microbiologica, et immunologica Scandinavica* **122**, 530-538

Downloaded from http://www.jbc.org/ by guest on July 16, 2017

30. Shin, J. O., Nakagawa, E., Kim, E. J., Cho, K. W., Lee, J. M., Cho, S. W., and Jung, H. S. (2012) miR-200b regulates cell migration via Zeb family during mouse palate development. *Histochemistry and cell biology* **137**, 459-470
31. Bellon, E., Luyten, F. P., and Tylzanowski, P. (2009) delta-EF1 is a negative regulator of Ihh in the developing growth plate. *The Journal of cell biology* **187**, 685-699
32. Gubelmann, c., Petra, C. S., and Deplancke, B. (2014) Identification of the transcription factor ZEB1 as a central component of the adipogenic gene regulatory network. *eLIFE* **3**, 1-30
33. Zhang, P., Wei, Y., Wang, L., Debeb, B. G., Yuan, Y., Zhang, J., Yuan, J., Wang, M., Chen, D., Sun, Y., Woodward, W. A., Liu, Y., Dean, D. C., Liang, H., Hu, Y., Ang, K. K., Hung, M. C., Chen, J., and Ma, L. (2014) ATM-mediated stabilization of ZEB1 promotes DNA damage response and radioresistance through CHK1. *Nature cell biology* **16**, 864-875
34. Darling, D. S., Stearman, R. P., Qi, Y., Qiu, M.-S., and Feller, J. P. (2003) Expression of Zfhep/δEF1 protein in palate, neural progenitors, and differentiated neurons. *Gene Expression Patterns* **3**, 709-717
35. Sabourin, J. C., Ackema, K. B., Ohayon, D., Guichet, P. O., Perrin, F. E., Garces, A., Ripoll, C., Charite, J., Simonneau, L., Kettenmann, H., Zine, A., Privat, A., Valmier, J., Pattyn, A., and Hugnot, J. P. (2009) A mesenchymal-like ZEB1(+) niche harbors dorsal radial glial fibrillary acidic protein-positive stem cells in the spinal cord. *Stem cells* **27**, 2722-2733
36. Thoma, E. C., Wischmeyer, E., Offen, N., Maurus, K., Siren, A. L., Schartl, M., and Wagner, T. U. (2012) Ectopic expression of neurogenin 2 alone is sufficient to induce differentiation of embryonic stem cells into mature neurons. *PloS one* **7**, e38651
37. Kim, T., Veronese, A., Pichiorri, F., Lee, T. J., Jeon, Y. J., Volinia, S., Pineau, P., Marchio, A., Palatini, J., Suh, S. S., Alder, H., Liu, C. G., Dejean, A., and Croce, C. M. (2011) p53 regulates epithelial-mesenchymal transition through microRNAs targeting ZEB1 and ZEB2. *The Journal of experimental medicine* **208**, 875-883
38. Jiang, H., Xu, Z., Zhong, P., Ren, Y., Liang, G., Schilling, H. A., Hu, Z., Zhang, Y., Wang, X., Chen, S., Yan, Z., and Feng, J. (2015) Cell cycle and p53 gate the direct conversion of human fibroblasts to dopaminergic neurons. *Nature communications* **6**, 10100
39. Liu, Y., Mukhopadhyay, P., Pisano, M. M., Lu, X., Huang, L., Lu, Q., and Dean, D. C. (2013) Repression of Zeb1 and hypoxia cause sequential mesenchymal-to-epithelial transition and induction of aid, Oct4, and Dnmt1, leading to immortalization and multipotential reprogramming of fibroblasts in spheres. *Stem cells* **31**, 1350-1362

Downloaded from http://www.jbc.org/ by guest on July 16, 2017

FIGURE LEGENDS:

FIGURE 1. *Zeb1* was strongly up-regulated during the early stages of transdifferentiation from MEFs into iN cells. (*A*) The mouse cDNAs of *Ascl1*, *Brn2*, *Ngn2* and *Zeb1* were cloned into a commercial adenoviral vector (pAd/CMV/V5-DEST^{TM}) under the control of a CMV promoter. (*B*) A schematic overview of the generation of iN cells by ABN or ABN + *Zeb1*. (*C*) iN cells were immunostained with TUJ1 on days 7, 14 and 21 post-infection. eGFP marks cells infected by adenovirus (here and for subsequent experiments). DAPI shows nuclei. Scale bar, 50 μm. (*D*) Western blot of ZEB1 and TUJ1 expression in the indicated cells. β-actin is the loading control (here and for subsequent experiments). (*E*) Quantitative real-time PCR analysis of *Zeb1* expression during ABN-induced transdifferentiation.

FIGURE 2. *Zeb1* shRNA strongly reduced the efficiency of ABN-induced transdifferentiation from MEFs into iN cells. (*A*) Western blot of ZEB1 in cells transfected with either control siRNA or *Zeb1* shRNA. (*B*) Immunofluorescence staining of TUJ1 in cells with indicated treatment. The immunostaining was repeated at least 3 times (here and for subsequent experiments). Scale bar, 50 μm. (*C*) The transdifferentiation efficiency from MEFs into iN cells was presented as the percentage of induced TUJ1-positive cells versus total cells stained by DAPI. Data represent the mean ± S.D. **, $P < 0.01$.

FIGURE 3. *Zeb1* overexpression promoted the generation of iN cells. (*A*) Immunofluorescence staining of TUJ1 in iN cells treated with different combinations for 7 days as indicated. Scale bar, 50 μm. (*B*) The transdifferentiation efficiency from MEFs into iN cells, presented as the percentage of ABN + empty vector (EV) or ABN + *Zeb1*-induced TUJ1-positive neuronal cells versus total cells 7-days post-infection. The total cells were determined by DAPI staining. Data represent the mean ± S.D. **, $P < 0.01$. (*C*) Western blot of ZEB1 expression in cells under the indicated treatments.

FIGURE 4. Characterization of iN cells by mature neuronal markers. Immunostaining analysis of mature neuronal markers two weeks post-infection using the antibodies against *Map2a* (*A*), *NeuN* (*B*) and *Synapsin* (*C*), pan-neuronal markers. *GAD67* (*D*), inhibitory neuron marker; Tyrosine hydroxylase (*TH*) (*E*), dopaminergic neuron marker; *vGLUT1* (*F*), excitatory neuron marker. Scale bar, 50 μm.

FIGURE 5. Identification of iN cells by electrophysiology. (*A*-*C*) Electrophysiology recordings of iN cells induced by ABN (*A*) or ABN + *Zeb1* (*B*) for 3 weeks. (*C*) Electrophysiology recordings of mouse primary neurons as a positive control. The Na^+ and K^+ current crest values are shown.

FIGURE 6. *Zeb1* overexpression promoted the generation of iN cells following transdifferentiation with A, B or N alone. (*A*-*C*) Immunofluorescence staining of TUJ1 in the indicated cells. The conversion efficiency of each group was quantified by calculating the ratio of TUJ1-positive cells versus the total cells. Data represent the means ± S.D. **, $P < 0.01$. Scale bars, 50 μm.

FIGURE 7. Transplantation of ABN + *Zeb1* iN cells *in vivo*. (*A*) A schematic overview of grafted GFP+ iN cells transplantation in the brain cortex. (*B*) iN cells express SYNAPSIN 3 weeks after transplantation. (*C*-*E*) iN cells express mature neuronal markers NeuN (*C*), GAD67 (*D*), vGLUT1 (*E*) 3 weeks after transplantation. Scale bars, 50μm.

FIGURE 8. Whole-genome RNA array analysis of gene expression profiles. (*A*) Hierarchical clustering analysis of the whole-genome profiles of ABN + *Zeb1* groups. Primary neurons were isolated from the hippocampus of a newborn pup. iN cells were harvested at the indicated time points. (*B*) Hierarchical clustering analysis of specific genes mainly expressed in neurons or MEFs. Primary neurons were isolated from the hippocampus of a newborn pup, as above. iN cells were derived 7-days post-transfection. (*C*) Venn diagram showing the overlap between the 6569 DEGs from the ABN group and the 6600 DEGs from the ABN + *Zeb1* group after 7 days of cultivation. (*D*) Gene ontology analysis of the significantly differentially expressed genes in the 7-day ABN + *Zeb1* group versus ABN.

Downloaded from http://www.jbc.org/ by guest on July 16, 2017

Figure. 1

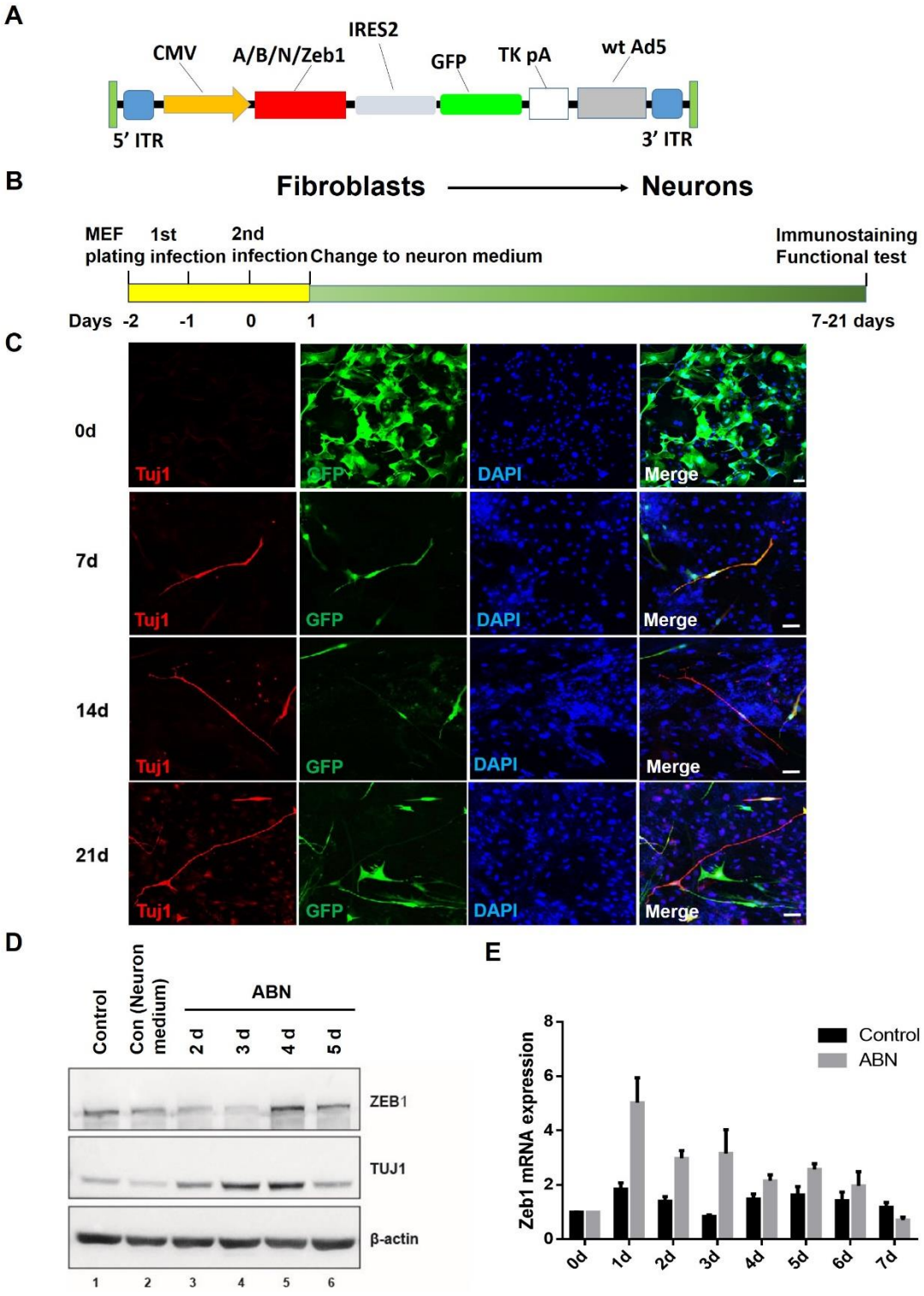

Downloaded from http://www.jbc.org/ by guest on July 16, 2017

Figure. 2

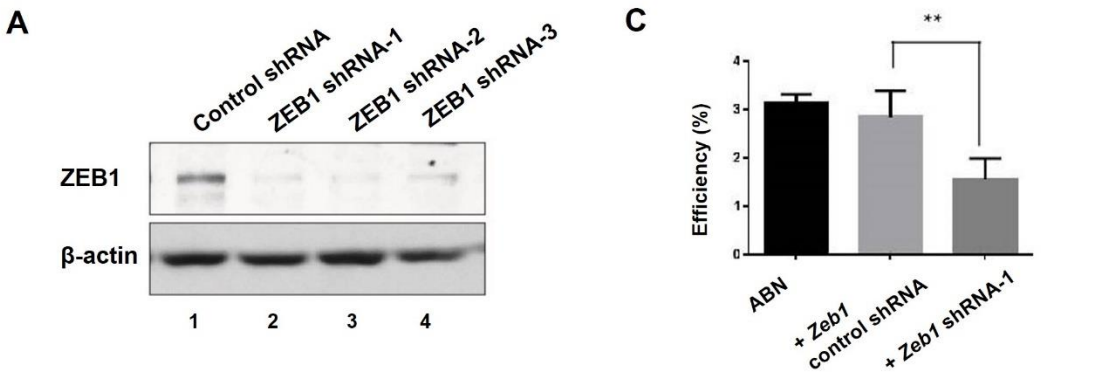

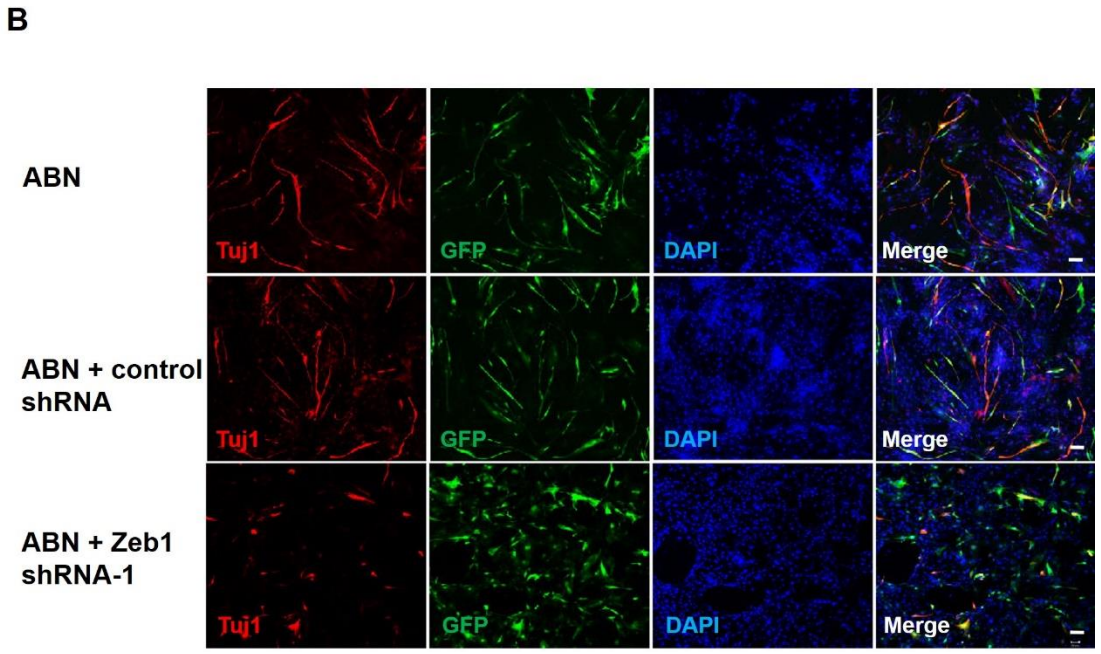

Downloaded from http://www.jbc.org/ by guest on July 16, 2017

Figure. 3

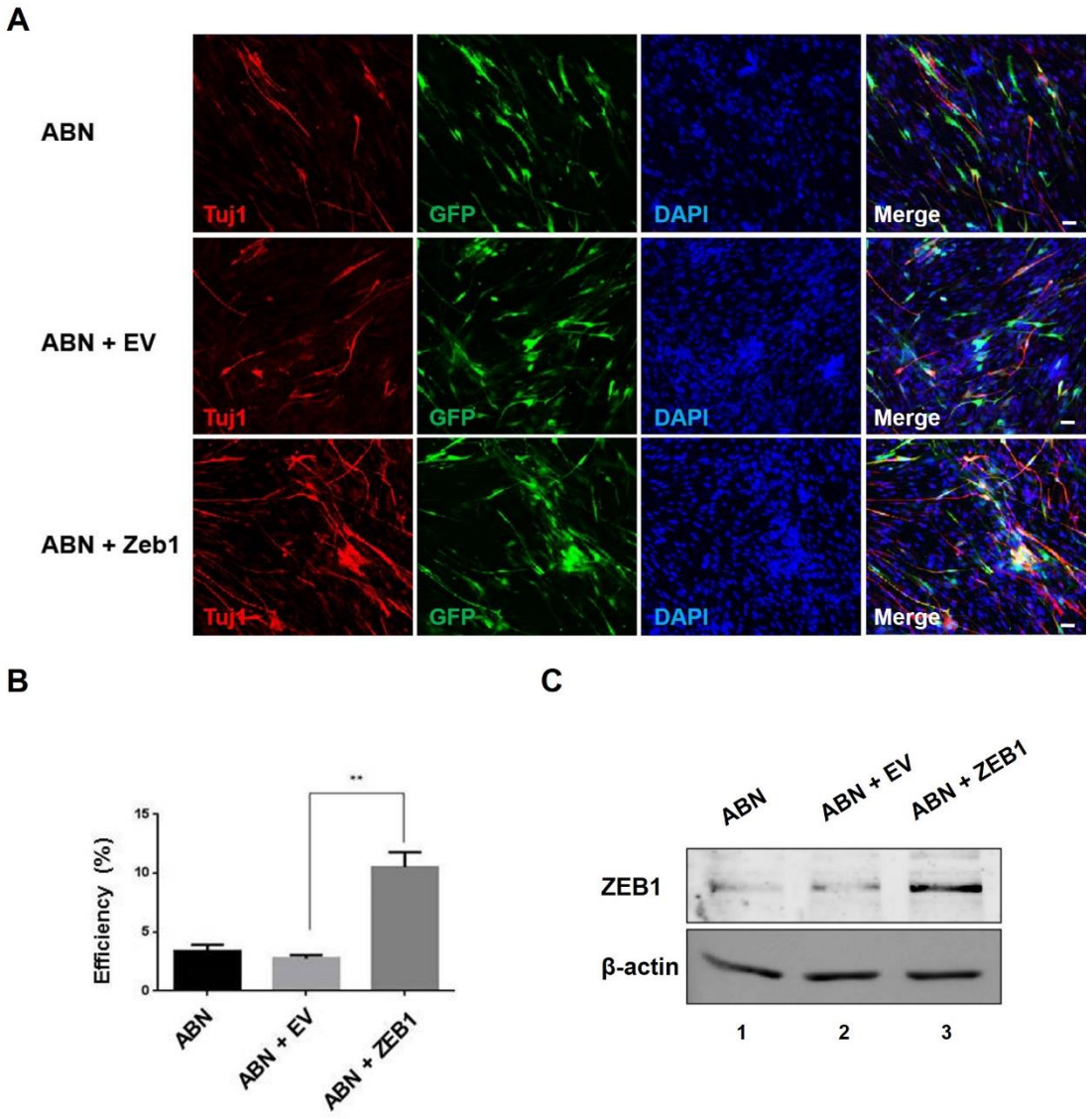

Downloaded from http://www.jbc.org/ by guest on July 16, 2017

Figure. 4

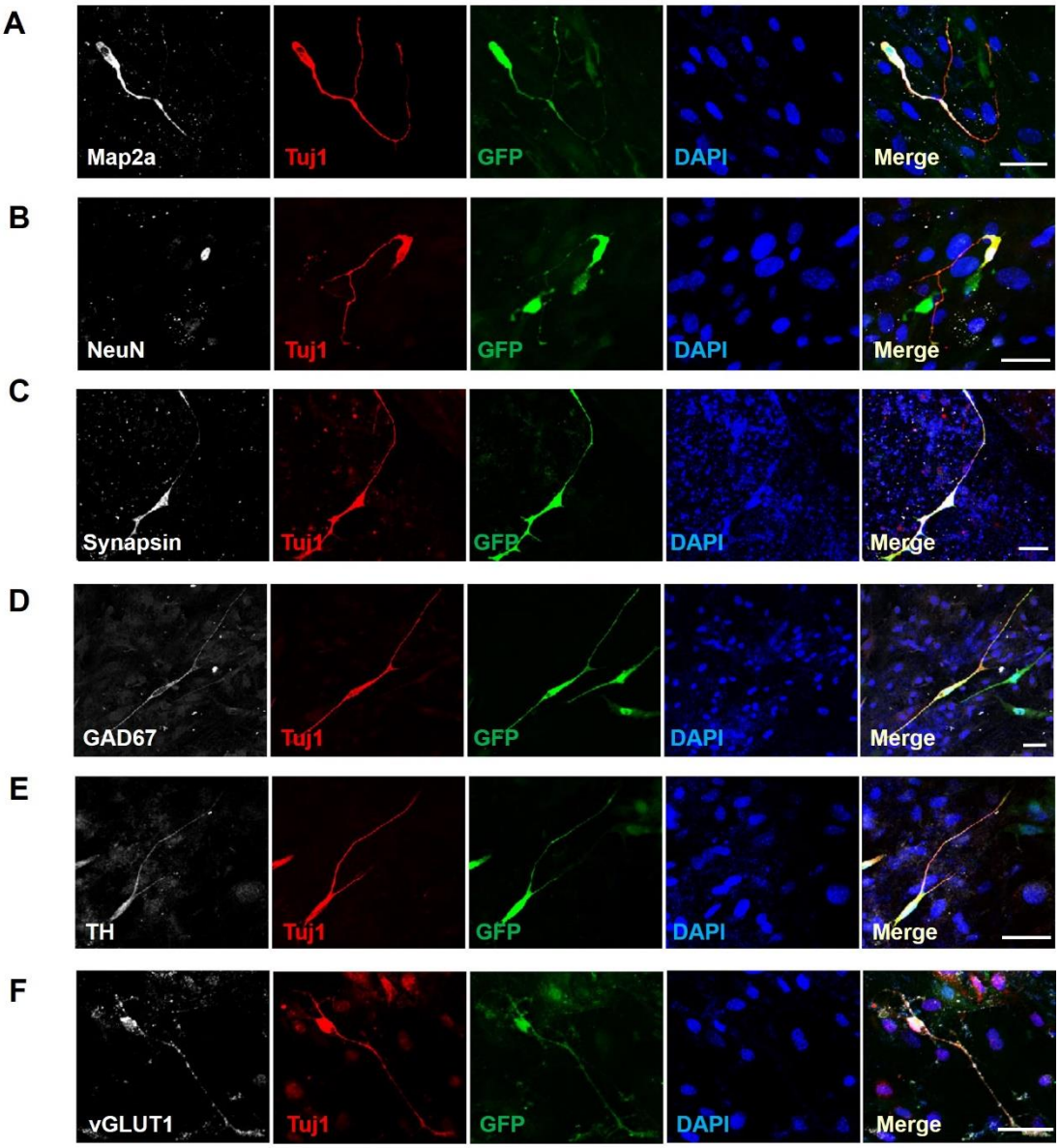

Downloaded from http://www.jbc.org/ by guest on July 16, 2017

Figure. 5

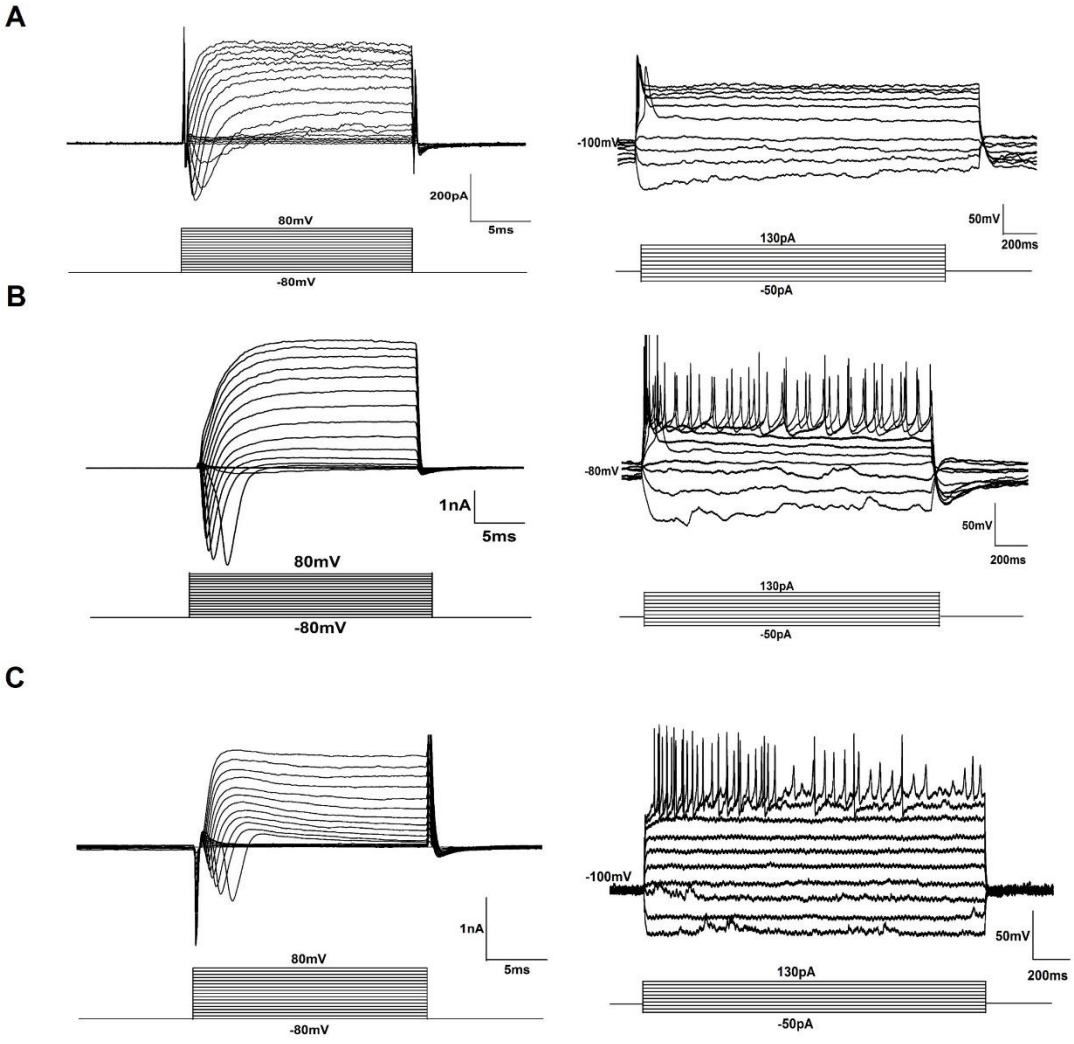

Downloaded from http://www.jbc.org/ by guest on July 16, 2017

Figure. 6

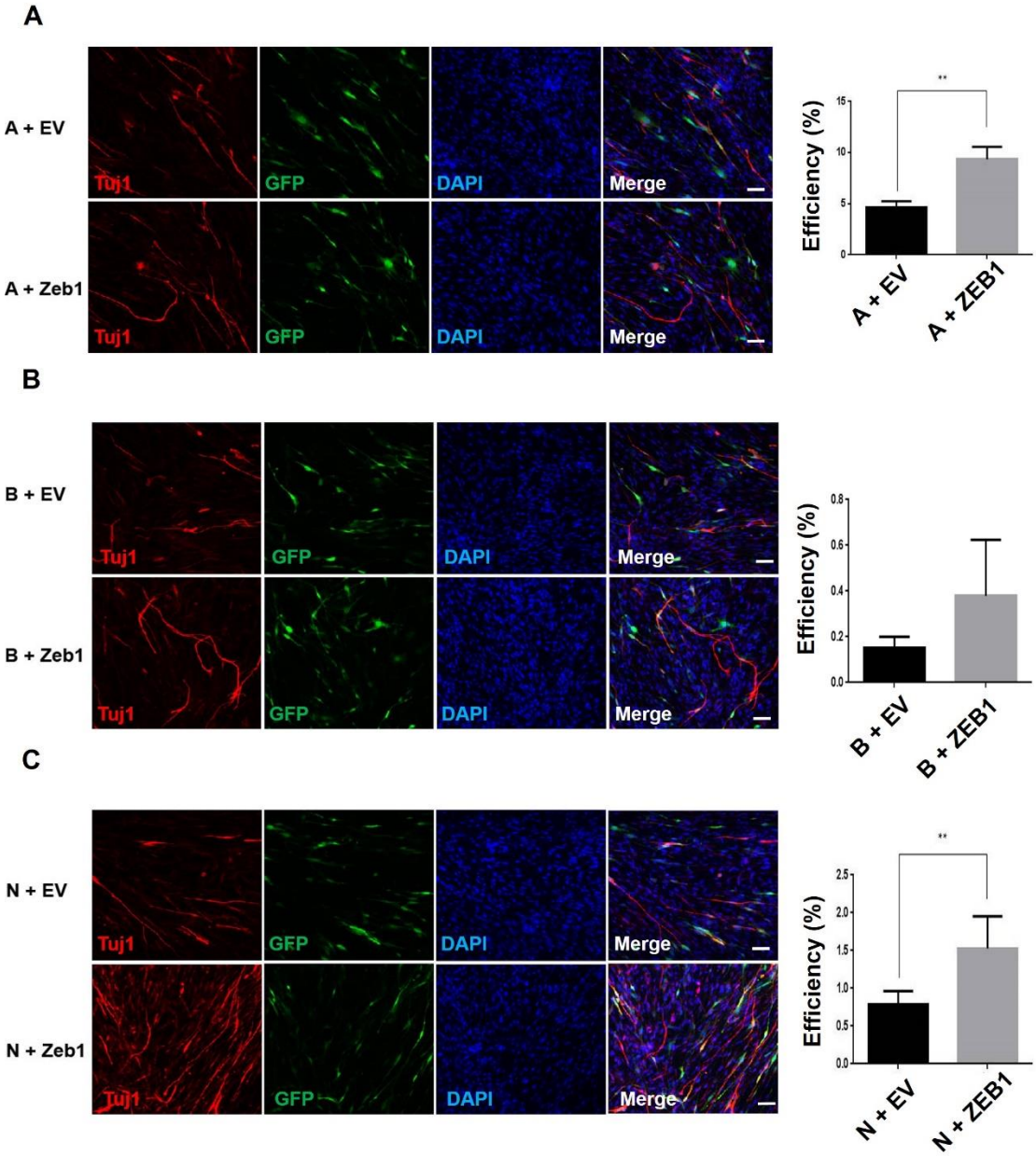

Downloaded from http://www.jbc.org/ by guest on July 16, 2017

Figure. 7

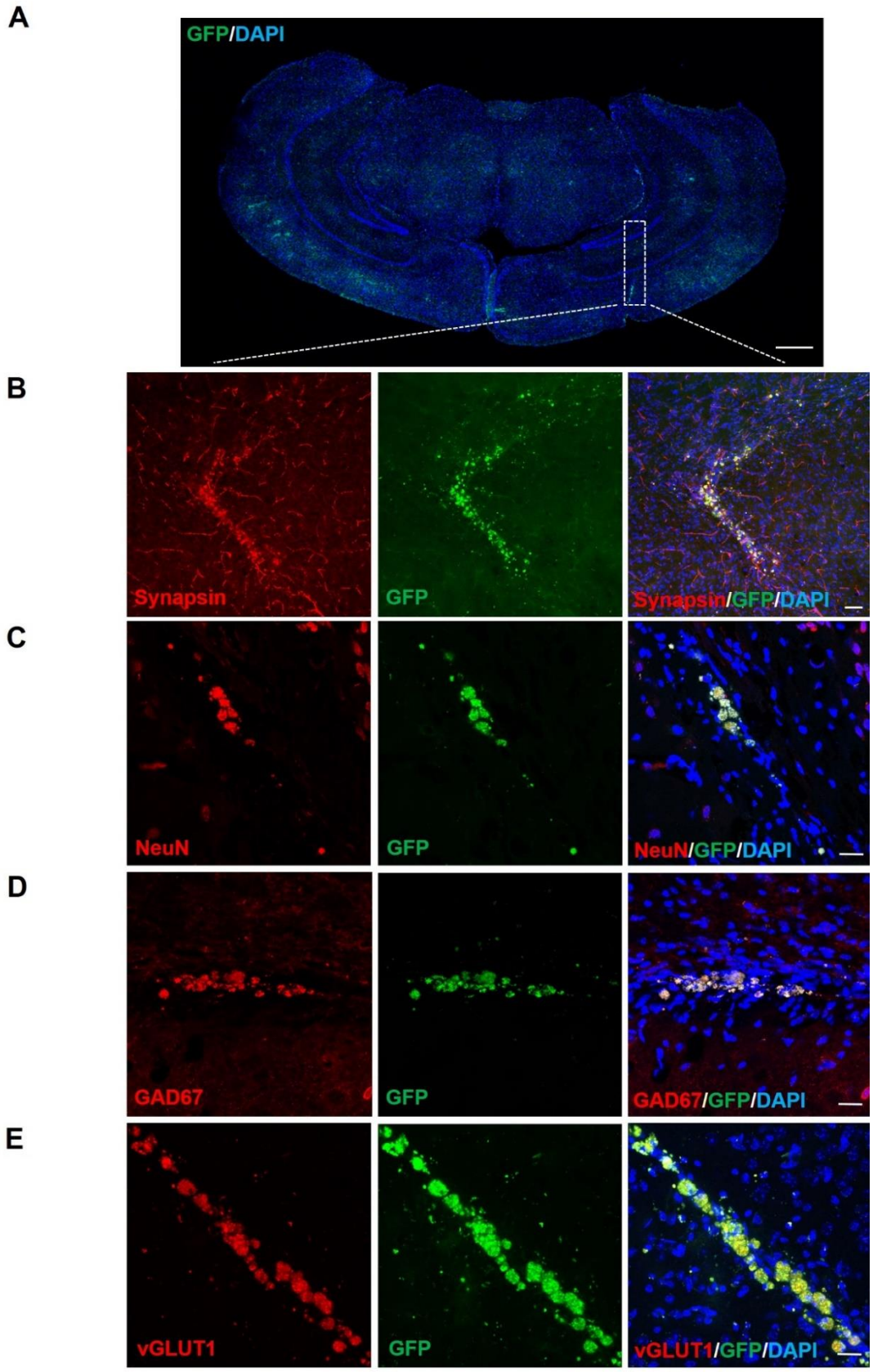

Downloaded from http://www.jbc.org/ by guest on July 16, 2017

Figure. 8

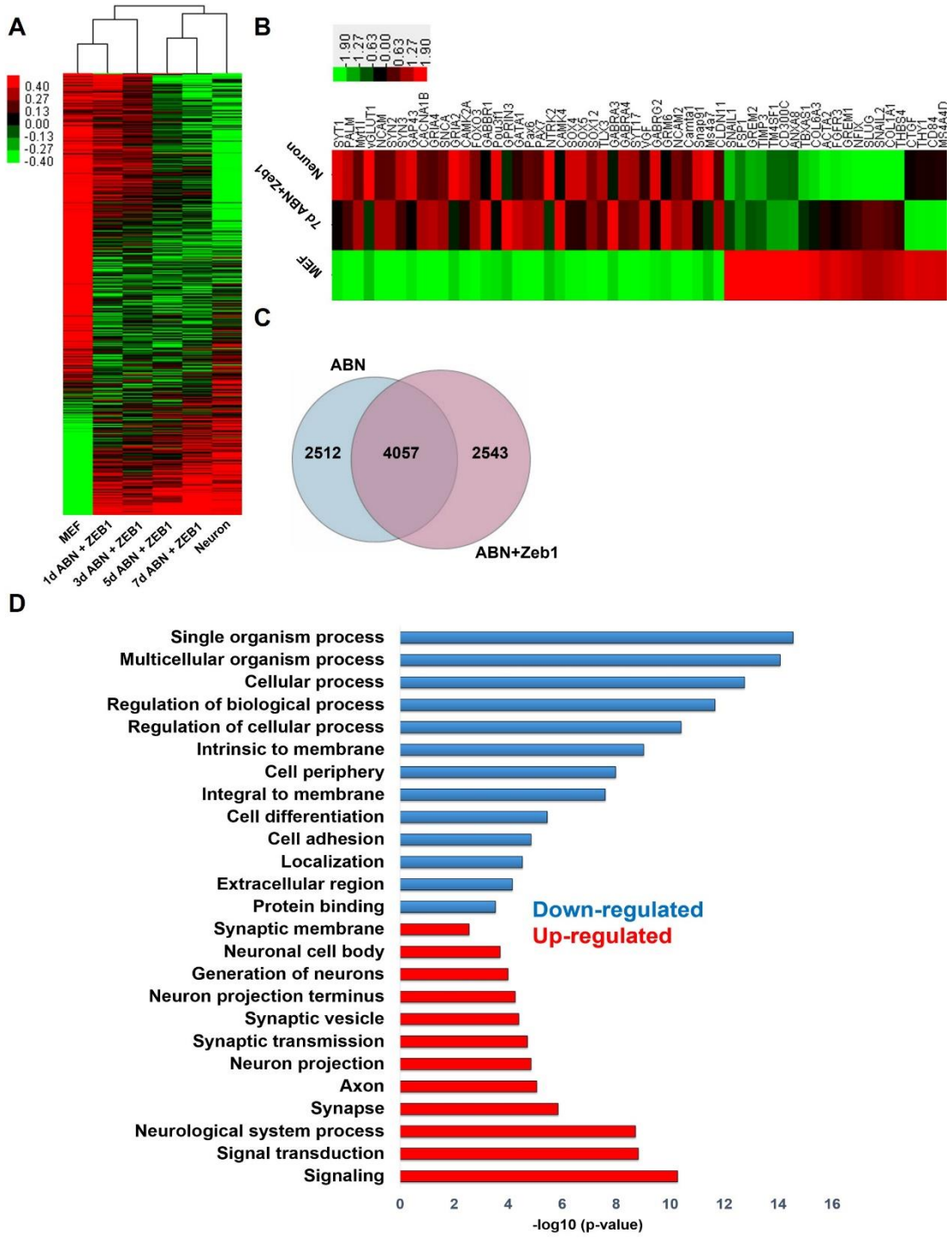

Downloaded from http://www.jbc.org/ by guest on July 16, 2017

The zinc finger E-box-binding homeobox 1 (Zeb1) promotes the conversion of mouse fibroblasts into functional neurons

Long Yan, Yue Li, Zixiao Shi, Xiaoyin Lu, Jiao Ma, Baoyang Hu, Jianwei Jiao and Hongmei Wang

J. Biol. Chem. published online May 12, 2017

Access the most updated version of this article at doi: 10.1074/jbc.M116.771493

Alerts:
- When this article is cited
- When a correction for this article is posted

Click here to choose from all of JBC's e-mail alerts

Supplemental material:
http://www.jbc.org/content/suppl/2017/05/12/M116.771493.DC1

This article cites 0 references, 0 of which can be accessed free at
http://www.jbc.org/content/early/2017/05/12/jbc.M116.771493.full.html#ref-list-1

Downloaded from http://www.jbc.org/ by guest on July 16, 2017